Barcelona '10

F024

Analysis of Seismicity Resulting from Time-dependent Fluid Injection Source Pressures

C. Dinske* (Free University of Berlin) & S.A. Shapiro (Free University of Berlin)

SUMMARY

Fluid induced seismicity is often governed by linear pressure diffusion. We relate the perturbed pore pressure to the induced seismicity to study the fluid - rock interaction, to examine physical processes and to characterize the reservoir. Solutions of the diffusion equation exist for the condition of constant source strength. But in some injection experiments, such as in Basel (Switzerland), the source strength is not constant over time. Here we present the solution of the diffusion equation which considers the special problem of linear rising source strength. Using the solution, we accordingly modify already established methods for a seismicity based reservoir characterization (SBRC). These methods are based on a statistical approach and consider features of induced seismicity such as the spatial event density and the seismicity rate. We apply those methods to the Basel microseismic data. Our analysis result in consistent estimates of hydraulic properties of the stimulated reservoir. We obtain a scalar permeability of around 75 microDarcy by assuming an effective isotropic medium. Furthermore, we study the criticality field which describes the strength of preexisting fractures in the reservoir. We observe that it is bounded by a minimum criticality of approximately 2000 Pa and a maximum criticality of about 0.75 MPa.

Introduction

Borehole fluid injections into surrounding rocks are used for development of hydrocarbon and geothermal reservoirs. Such injections are often accompanied by microseismic activity. Despite the nature of fluid induced seismicity is still topic of ongoing research, one hypothesis argues that triggering of this type of seismicity is controlled by a diffusion process of relaxation of a pressure perturbation (Shapiro et al., 1997). If assuming that stresses in the Earth crust are in sub-critical condition then minor changes of the stress state can already cause seismicity. Due to injection of fluid the pore pressure increases which consequently decreases the effective normal stress. It leads to reactivation of preexisting faults and fractures by triggering slip events and thereby releasing previously accumulated shear stress in the stimulated rock volume (Rutledge and Phillips, 2003). Based on the concept of pressure diffusion, *SBRC* (Seismicity Based Reservoir Characterization) methods were introduced (e.g. Shapiro et al., 2003, 2005). Analysis of spatio-temporal dynamics of fluid induced seismicity and comparison with numerical modeling support the above hypothesis and contribute to a better understanding of the physical processes. Typical signatures confirming the diffusive nature are, for example, triggering front and back front of seismicity. Further evidences are related to seismicity rate, event density, criticality reconstruction and magnitude characteristics. In general, *SBRC* methods can be used to estimate hydraulic properties of the stimulated reservoir. Some of above methods are directly linked with the solution of the diffusion equation (Carslaw and Jaeger, 1973). In those cases, the condition of a constant injection pressure is assumed. However, in situations where this condition does not meet the design parameters of an injection experiment usage of these *SBRC* methods produce inaccurate results. It applies to, for example, the Basel reservoir stimulation in 2006 where flow rates were stepwise increased which caused an injection pressure build-up from $10\ MPa$ to $30\ MPa$ (Häring et al., 2008). *SBRC* methods therefore require modification to account for non-constant source pressure.
Here we present the solution of the diffusion equation which considers the special problem of a (linear) rising injection source strength. The solution is used to accordingly adapt *SBRC* methods that we apply to the Basel microseismic data. Thus, we can determine the hydraulic diffusivity of the reservoir and we can characterize the criticality field which describes the strength of preexisting fractures.

Pore pressure perturbation by rising injection source strength

First attempts to physically describe the nature of fluid induced seismicity and its triggering process were evaluated by Shapiro et al. (1997): Its spatio-temporal evolution is governed by a diffusion process of relaxation of pore pressure perturbation. In the most simplest case, that is to consider a homogenous isotropic fluid-saturated medium, the linear diffusion equation in 3D is $\frac{\partial p(r,t)}{\partial t} = D\nabla^2 p(r,t)$ with hydraulic diffusivity D and distance to the source point r. Generally, a solution of this equation has the form (Carslaw and Jaeger, 1973):

$$p(r,t) = \frac{1}{8(\pi D)^{3/2}} \int_0^t \psi(\tilde{t}) e^{\frac{-r^2}{4D(t-\tilde{t})}} \frac{d\tilde{t}}{(t-\tilde{t})^{3/2}}. \tag{1}$$

The source variable can be written as $\psi(t) = q_0 + q_t t$ with q_0 being a time-independent constant source strength, which can also be zero, and q_t being a constant rate of source strength increase. The source strength $\psi(t)$ is thus a linear rising function. Solving the integral, we obtain for the pore pressure perturbation $p(r,t)$:

$$p(r,t) = (\frac{q_0 + q_t t}{4\pi D r} + \frac{q_t r}{8\pi D^2}) \cdot erfc(\frac{r}{\sqrt{4Dt}}) - \frac{q_t\sqrt{t}}{4(\pi D)^{3/2}} \cdot exp(\frac{-r^2}{4Dt}) \tag{2}$$

where $erfc(z)$ is the complementary Gaussian error function. In the case of a finite injection source switched off at time t_0 the solution of the diffusion equation for times $t > t_0$ becomes:

$$\begin{aligned} p(r, t > t_0) = {} & (\frac{q_0 + q_t t}{4\pi D r} + \frac{q_t r}{8\pi D^2}) \cdot erfc(\frac{r}{\sqrt{4Dt}}) - \frac{q_t\sqrt{t}}{4(\pi D)^{3/2}} \cdot exp(\frac{-r^2}{4Dt}) \\ -[(\frac{q_0 + q_t(t-t_0) + q_t t_0}{4\pi D r} & + \frac{q_t r}{8\pi D^2}) \cdot erfc(\frac{r}{\sqrt{4D(t-t_0)}}) - \frac{q_t\sqrt{t-t_0}}{4(\pi D)^{3/2}} \cdot exp(\frac{-r^2}{4D(t-t_0)})] \end{aligned} \tag{3}$$

Both equations (2) and (3) fully describe the propagation of a pore pressure perturbation in a 3D volume caused by a fluid pressure source of rising strength and finite time. We have modified the *SBRC* methods which consider spatial event density, seismicity rate and cumulative event number using the derived solutions. They are based on the statistical approach that the probability of event triggering is directly proportional to the pore pressure perturbation, $W_{ev} = p(r,t)/dC$ (e.g. Shapiro et al., 2005). $dC = C_{max} - C_{min}$ is related to the criticality field $C(r)$ defining the fracture strength with C_{max} the maximum criticality (most stable) and C_{min} the minimum criticality (most unstable). In such a way, expressions for the seismicity rate $R(t)$ and the number of events $N_{ev}(t)$ can be obtained by solving following integrals:

$$R(t) = \frac{4\pi\zeta}{dC}\int_a^b r^2 \cdot \frac{\partial p(r,t)}{\partial t} dr \qquad\qquad N_{ev}(t) = \frac{4\pi\zeta}{dC}\int_a^b r^2 p(r,t) dr, \tag{4}$$

where ζ is the number of preexisting fractures. The integration limits a and b are defined by the time-dependent seismically active rock volume.

Case study - Basel Geothermal Reservoir

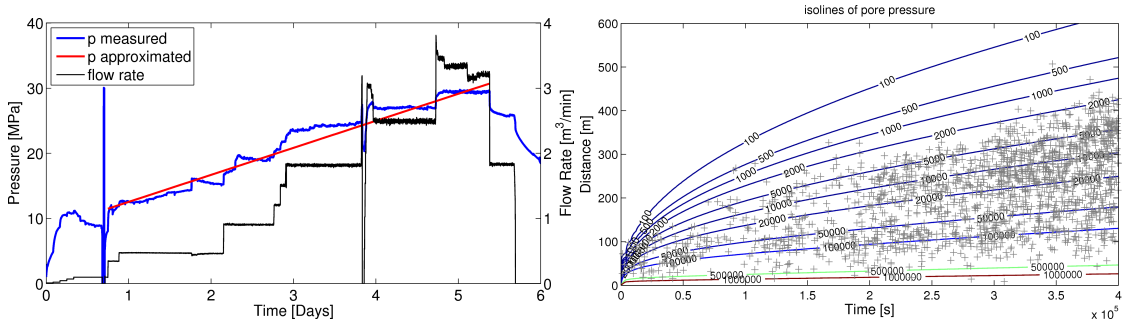

Figure 1 *(Left) Flow rates and injection pressures of the Basel reservoir stimulation. Red line shows rising pressure function with $p_0 = 11.5\ MPa$ and $p_t = 48\ Pa/s$ (obtained by linear regression). Begin and end of red line mark the considered time interval in our analysis. (Right) $r-t$ diagram of microseismic events (grey crosses) along with pore pressure isolines.*

In December 2006, a hydraulic stimulation of the geothermal reservoir in Basel (Switzerland) was performed to enhance the permeability. Within six days, about $11,500\ m^3$ water were pumped with stepwise increased flow rates up to $60\ l/s$ and a maximum wellhead pressure of $\sim 30\ MPa$ (Figure 1). During the period of injection, more than 10,000 microseismic events were detected and about 2,300 events could be located (Dyer et al., 2008).

For our analysis, we have adjusted the microseismic data to account for detected hydraulic anisotropy. Source coordinates of events are rotated and scaled to transfer the cloud into an equivalent cloud which would have been obtained under isotropic conditions (see Shapiro et al., 2003). Figure 1 shows the rotated and scaled event cloud in the space - time domain. In addition, isolines of pore pressure perturbation are illustrated. The pore pressure $p(r,t)$ is calculated according to equations (2) and (3). Source terms are given as $q_0 = 4\pi D a_0 p_0$ and $q_t = 4\pi D a_0 p_t$ with constant pressure $p_0 = 11.5\ MPa$, pressure gradient $p_t = 48\ Pa/s$, effective injection source radius $a_0 = 1\ m$, hydraulic diffusivity $D = 0.06\ m^2/s$ and injection time $t = 400,000\ s$, covering the time interval of significant and non-decreasing flow rates (Figure 1). The combined presentation of seismicity and pore pressure field allows to characterize the criticality field. In our model, the critical pressure $C(r)$ defines the pore pressure value which must be exceeded in a given point of the medium r to trigger an event. Pore pressures below the threshold value C_{min} are not sufficient to induce seismic events. On the other hand, the isoline of pore pressure with the value of maximum criticality corresponds to the distance below which all fractures have already ruptured and no further events can be triggered. It is evident from the $r-t$ diagram that during injection the upper envelope of microseismic events roughly coincides with the pore pressure isoline $2000\ Pa$ (Figure 1). Furthermore, a region of seismic inactivity below the isoline $0.5\ MPa$ can be identified. Both envelopes provide estimates of the controlling parameters of the seismically active volume during injection, that are $C_{min} \sim 2000\ Pa$ and $C_{max} \sim 0.5\ MPa$. However, the accuracy

of the result is influenced by location uncertainties and event catalog incompleteness due to magnitude detection threshold. For the following consideration we therefore limit the data by introducing a cut-off magnitude $M_w = 0.5$ that is defined from the frequency-magnitude distribution (see Dinske et al., 2009). To determine the spatial event density distribution, we follow the statistically approach proposed

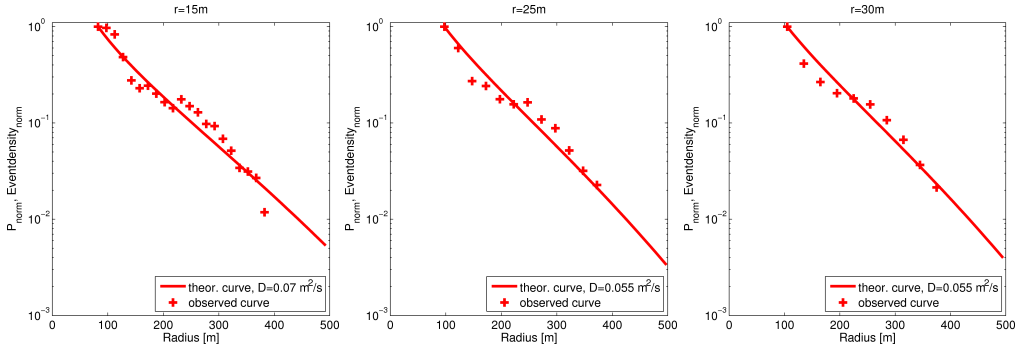

Figure 2 *Observed spatial event density as function of distance to injection point for different shell radii:* $15\ m$, $25\ m$ *and* $30\ m$ *(from left to right). Red curves are normalized pore pressures according to Equation (2).*

by Shapiro et al. (2005). Events are counted in concentric spherical shells centred at the injection point. The resulting event numbers are scaled by their respective shell volumes and then normalized to the scaled event number of the first shell. In the next step, the diffusivity D in Equation (2) is varied to correlate the pore pressure perturbation with the observed spatial density (Figure 2). Depending on the selected shell radius, we obtain best matches for hydraulic diffusivity ranging from $D = 0.055\ m^2/s$ to $D = 0.07\ m^2/s$.

In contrast to the event density, which can only be determined for localized events, we consider the catalog of detected events for an analysis of seismicity rate and cumulative event number. Figure 3 shows observed and theoretical seismicity rate each normalized to $t = t_0 = 400,000\ s$. The bars represent number of events per one hour which were detected during injection plus approximately nine days subsequent to the shut-in. The theoretical curve is calculated using diffusivity and criticality values that provide most-suitable correlation with the observation. Thus, we get a hydraulic diffusivity $D = 0.065\ m^2/s$, and minimum and maximum criticality are $C_{min} = 2500\ Pa$ and $C_{max} = 0.75\ MPa$, respectively. However, we notice deviations between observed and calculated seismicity rate. In particular, there are more predicted than triggered events during the first half of injection. But, if we additionally plot the flow rates one can see that seismicity triggering reacts very sensitive to the applied flow rate. Moreover, the two rates run nearly parallel if both are normalized to time $t = 400,000\ s$. The cumulative number of events along with the injected fluid volume show a similar behavior Figure 3. Nevertheless, prediction and observation well coincide in the post-injection phase. We therefore consider the cumulative event number after shut-in of the injection for a reservoir characterization. (Note that shut-in time is at about $430,000\ s$, see Figure 1). The decay characteristic of detected events requires an examination in two separate time windows (Figure 4). The theoretical cumulative event number for the first time interval is calculated with diffusivity $D = 0.055\ m^2/s$ and minimum criticality $C_{min} \sim 4300\ Pa$. For the second time window, the best fit is provided by the same diffusivity but the minimum criticality is $C_{min} = 1500 Pa$.

Discussion and Conclusions

We have presented the solution of the diffusion equation which is valid for the condition of linear rising source strength. We have then applied modified *SBRC* methods to obtain estimates for hydraulic diffusivity of the stimulated geothermal reservoir in Basel. The different methods provide consistent results which also agree with results we get using the heuristic approach of triggering fronts and from the empirically based Omori type analysis (not shown here). The diffusivity is proportional to the Darcy permeability, $K = \frac{\eta}{N} D$, which is in the order of $75\ microDarcy$. Häring et al. (2008) give a value of

10 $microDarcy$ for the rather undisturbed near-borehole area estimated from hydraulic data analysis. Furthermore, we have evaluated the strength of preexisting fractures in the reservoir. The strength is defined by a criticality field whose upper bound is below the maximum of pore pressure perturbation. Using numerical modeling, it can be shown that such a situation results in an increase of the size of induced events even after injection stop. This phenomenon is indeed observed in Basel where events with largest magnitudes occurred after shut-in (Häring et al., 2008). For the lower bound of criticality we obtain rather a range of estimates than one precise value. In fact, we get $C_{min} \sim 2000\ Pa$ if we only consider the injection period whereas C_{min} is between $1500\ Pa$ and $4300\ Pa$ if we consider the post-injection period. Possibly, this observation can be attributed to the two different sets of preexisting fractures as reported by Dyer et al. (2008). Depending on their alignment with respect to the direction of maximum horizontal stress, the two fracture systems can be characterized by different criticality fields.

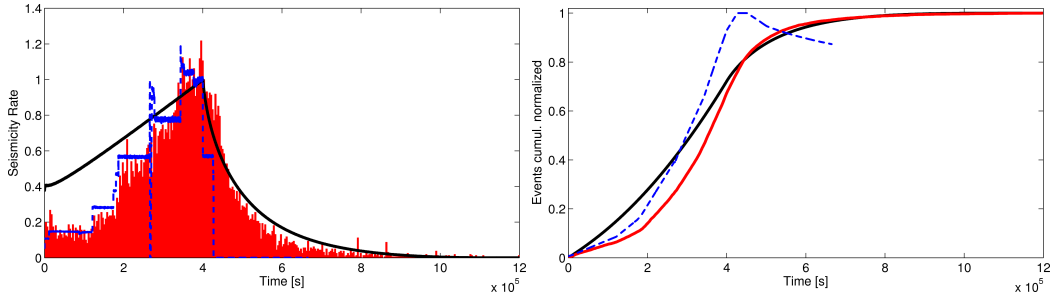

Figure 3 *(Left) Normalized seismicity rate (red bars: number of detected events per hour, black line: calculated seismicity rate, dashed blue line: fluid flow rates). (Right) Normalized cumulative number of events (red line: observed event number, black line: calculated event number, dashed blue line: injected fluid volume).*

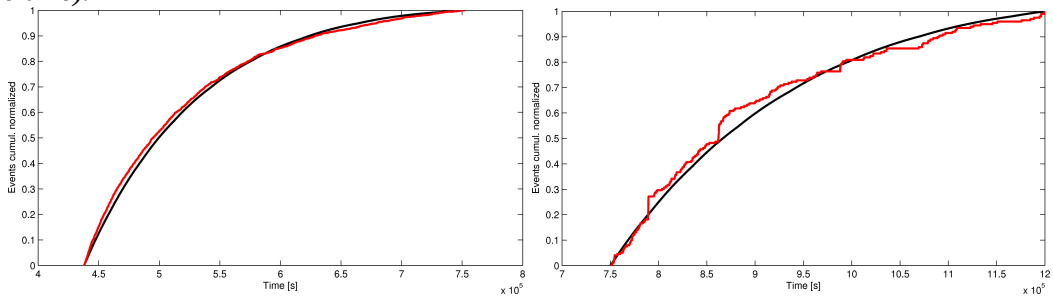

Figure 4 *Normalized cumulative number of events induced after shut-in (red line: observed number, black line: calculated number). To achieve good correlation between prediction and observation we consider two time intervals,* $438,000\ s$ *-* $750,000\ s$ *(left) and* $750,000\ s$ *-* $1.2 \cdot 10^6\ s$*.*

Acknowledgments

We thank the sponsors of the *PHASE consortium* for supporting the research presented in this paper. The Basel data are kindly provided by Dr. Häring and are courtesy of Geothermal Explorers.

References

Carslaw, H.S. and Jaeger, J.C. [1973] *Conduction of heat in solids*. Oxford University Press, London.

Dinske, C., Shapiro, S.A. and Ladner, F. [2009] Seismicity based reservoir characterization of basel geothermal site. *71st EAGE Conference Expanded Abstracts*, Amsterdam, paper–P033.

Dyer, B.C., Schanz, U., Spillmann, T., Ladner, F. and Häring, M.O. [2008] Microseismic imaging of a geothermal reservoir stimulation. *TLE*, **27**(7), 856–869.

Häring, M.O., Schanz, U., Ladner, F. and Dyer, B.C. [2008] Characterisation of the Basel 1 enhanced geothermal system. *Geothermics*, doi:10.1016/j.geothermics.2008.06.002.

Rutledge, J.T. and Phillips, W.S. [2003] Hydraulic stimulation of natural fractures as revealed by induced microearthquakes, Carthage Cotton Valley gas field, east Texas. *Geophysics*, **68**, 441–452.

Shapiro, S.A., Huenges, E. and Borm, G. [1997] Estimating the permeability from fluid-injection induced seismic emission at the KTB site. *Geophys J Int*, **131**, F15–F18, see also Corrigendum, Geophys J Int, 134, 913.

Shapiro, S.A., Patzig, R., Rothert, E. and Rindschwentner, J. [2003] Triggering of seismicity by pore-pressure perturbations: permeability-related signatures of the phenomenon. *Pure Appl Geophys*, **160**, 1051–1061.

Shapiro, S.A., Rentsch, S. and Rothert, E. [2005] Characterization of hydraulic properties of rocks using probability of fluid-induced microearthquakes. *Geophysics*, **70**, F27–F33.